(17) Boue, F.; Nierlich, M.; Leibler, L. *Polymer* **1982**, *23*, 19.
(18) Crist, B. W.; Graessley, W. W.; Wignall, G. D. *Polymer* **1982**, *23*, 1561.
(19) Altgelt, K.; Schultz, G. V. *Makromol. Chem.* **1960**, *36*, 209.
(20) Flory, P. J. "Statistical Mechanics of Chain Molecules"; Wiley-Interscience, New York, 1969; pp 191-2.
(21) Wignall, G. D.; Mandelkern, L.; Edwards, C.; Glotin, M. *J. Polym. Sci., Phys. Ed.* **1982**, *20*, 245.
(22) Fisher, E. W.; Stamm, M.; Dettenmaier, M., Herschenroeder, P. *Polym. Prepr., Am. Chem. Soc., Div. Polym. Chem.* **1979**, *20*, 219.
(23) Ballard, D. G. H.; Cheshire, P.; Longman, G. W. *Polymer* **1978**, *19*, 379.
(24) Wu, W. L.; Wise, D.; Zachmann, H. G.; Hahn, D. *Bull. Am. Phys. Soc.* **1984**, *29*, 241.
(25) We have recently performed experiments with newly synthesized PET-D in which the 100% PET-D sample scattering has been reduced by 1 order of magnitude. The value of $R_g/M_w^{1/2}$ obtained with this material is 0.376. As this is almost identical with the average value of 0.373 reported in this paper, we believe that the subtraction method used in our calculations is valid.

Simulation of Small-Angle Neutron Scattering from Microphase-Separated Block Copolymers

R. W. Richards* and J. L. Thomason†

Department of Pure and Applied Chemistry, University of Strathclyde, Glasgow G1 1XL, U.K. *Received October 26, 1983*

ABSTRACT: The small-angle neutron scattering from microphase-separated block copolymers has been simulated on the basis of three major components to the scattered intensity: the single-particle form factor scattering from individual domains, interference function scattering from domain long-range order, and incoherent background scattering. Single-particle form factor scattering may be treated independently of the interference function and special attention has been paid to the use of partly deuterated copolymers and the influence of the orientation of anisometric domains on the scattered intensity. Orientation is found to have a severe influence on the scattered intensity. A comparison is made with experimental data and the agreement is fair. The interference function scattering has been modeled by a paracrystalline lattice modulated by the single-particle form factor scattering from which it is inseparable. Calculation of interference function scattering has been simplified by using a one-dimensional equivalent lattice and adjusting parameters systematically. Comparison with experimental data is reasonable in that the correct positions of the Bragg peaks are obtained, although calculated peaks are narrower and of greater amplitude. The agreement between model and experiment lends support to our conclusion that spherical domains in styrene–isoprene block copolymers are organized on an approximately face-centered cubic lattice. Detector resolution and wavelength distribution are also included while incoherent background is calculated on a relative basis.

Introduction

Microphase separation is a fundamental feature of the solid-state structure of styrene–isoprene block copolymers.[1] Microphase-separated domain morphology has been discussed from a statistical thermodynamics viewpoint and the composition ranges for equilibrium morphologies have been identified.[2-4] Concurrent with theoretical studies have been experimental investigations of block copolymer solid state; for present purposes small-angle scattering studies are of greatest moment. Of particular note is the work of Hashimoto[5-8] dealing with the small-angle X-ray scattering (SAXS) of these copolymers in the solid state and in concentrated solution. Recently, small-angle neutron scattering (SANS) results have been published by us and others.[9-14] The advantages of SANS derive from the prospect of selective labeling; however, major disadvantages are the lower resolution of SANS detectors and the lower signal-to-noise ratio due to incoherent neutron scattering from protons. These two disadvantages assume a greater or lesser importance depending on the scattering vector ($\mathbf{Q}$) range investigated. Thus, low resolution broadens Bragg peaks observed at low Q and hinders assignment of long-range structure. At higher Q values, the relatively large background scattering can prevent observation of single-domain scattering and must be carefully accounted for in the analysis of domain–matrix boundaries.

At small scattering vectors, the diffraction patterns from styrene–diene block copolymers are dominated by distinct maxima, Bragg peaks, arising from the long-range order of domains. At higher Q values one or more broad maxima of considerably smaller amplitude may be observed before the intensity decays to a featureless attenuation with increasing Q until an asymptotic intensity is obtained. The broad maxima arise from single-domain scattering while an accelerated attenuation with Q is characteristic of the domain boundary.

Analysis of such diffraction patterns in terms of a structure is often difficult. The Bragg maxima tend to be broad and ill-resolved with absences of expected maxima for particular structures. Single-domain scattering is weak and is weakened still further by the presence of even a modest distribution in domain size. The influence of domain size distribution and a diffuse interface has been discussed by Hashimoto[5-7] especially for spherical domains. Other factors which may be of importance are the domain orientation, for lamellar and cylindrical symmetries, and the level of background scattering.

We report here an attempt to model the SANS from block copolymers using a Fortran package which permits the inclusion of instrumental factors (e.g., wavelength distribution, detector resolution) as well as factors associated with the block copolymers (e.g., domain size, domain spacing, and distributions in these). The approach used is semiempirical in that known scattering laws are used as starting points and the influence of the various factors on them is noted. Finally, the results are compared with experimental data.

Fundamental Equations

A detailed discussion of the equations relating to SANS of block copolymers has been given elsewhere.[10] A brief

† Present address: Koninklijke/Shell-Laboratorium, 1003 AA Amsterdam, The Netherlands.

0024-9297/85/2218-0452$01.50/0

restatement only is given here so that important terms can be identified; all symbols used are defined in the Glossary of Symbols.

Equation 1 defines the intensity of elastically scattered

$$I(\mathbf{Q}) = K[(d\sigma_c/d\Omega) + \sigma_{inc}/4\pi] \quad (1)$$

neutrons per second by any material and $\sigma_{inc}/4\pi$ is the incoherent background scattering. The differential coherent scattering cross section, $d\sigma_c/d\Omega$, retains all the phase information of the scattered neutrons. Using a two-phase model and assuming centrosymmetric scattering particles then

$$d\sigma_c/d\Omega = (C_f V_p^2 N_p/N)\langle F_p(\mathbf{Q})\rangle^2 A(Q) \quad (2)$$

whence

$$I(\mathbf{Q}) = K[(C_f V_p^2 N_p/N)\langle F_p(\mathbf{Q})\rangle^2 A(Q) + \sigma_{inc}/4\pi] \quad (3)$$

The single-particle form factor (SPFF), $\langle F_p(\mathbf{Q})\rangle^2$, is determined by the domain morphology and size. The interference function, $A(Q)$, is a characteristic of correlations between domains and is formally identified with a liquid structure factor. However, there is always a region of Q where $A(Q) = 1$ and $I(\mathbf{Q})$ is determined by the SPFF alone.

Referring to eq 3, it is evident that the interference function cannot be factorized from the SPFF and is always modulated by this parameter. Because the SPFF can be observed independently, then we discuss this and the influence of various factors on it before the interference function scattering.

Single-Domain Scattering

For the domain morphologies encountered in styrene–diene block copolymers, the SPFFs are given by

sphere[15]

$$F_p^2(\mathbf{Q}) = [9\pi/2(QR_s)^3]J_{3/2}^2(QR_s) \quad (4)$$

cylinder[16]

$$F_p^2(\mathbf{Q}) = [4/(QR_c)^2]J_1^2(QR_c) \quad (5)$$

lamella[10]

$$F_p^2(\mathbf{Q}) = [\pi/QL]J_{1/2}^2(QL/2) \quad (6)$$

Factors associated with either technique or specimen which may influence the scattered intensity to a greater or lesser degree include (1) detector resolution, (2) wavelength distribution of the incident neutron beam, (3) multiple scattering, (4) domain size distribution, (5) diffuse domain–matrix boundary, (6) ratio of signal to noise, i.e., the level of incoherent scattering, and (7) anisometric domain orientation.

Some of these factors have been discussed in relation to other problems by others and a detailed consideration of their inclusion in the model is not provided. Multiple scattering has been shown to have severe influence on the resolution of SPFF scattering;[17] however, Goyal et al.[18] have shown that its occurrence in SANS from polymers is negligible. Our experimental results[9,10] on styrene–isoprene block copolymers confirm the insignificance of multiple scattering. Domain size distribution and diffuse domain boundary have been modeled by Hashimoto et al.[6] for spherical domains. Increasing the width of the domain size distribution severely weakens the maxima in the SPFF but does not shift their Q positions from those pertaining to monodisperse domains. Incorporating a diffuse domain–matrix boundary accelerates the attenuation of intensity with Q as expected. These features have been included in the model discussed by using a normalized Gaussian distribution of domain sizes, whose width is defined by a standard deviation, and using Ruland's[11-19] equations for the Fourier transform of the smoothing function reproducing Helfand's[2] density variation across the interface.

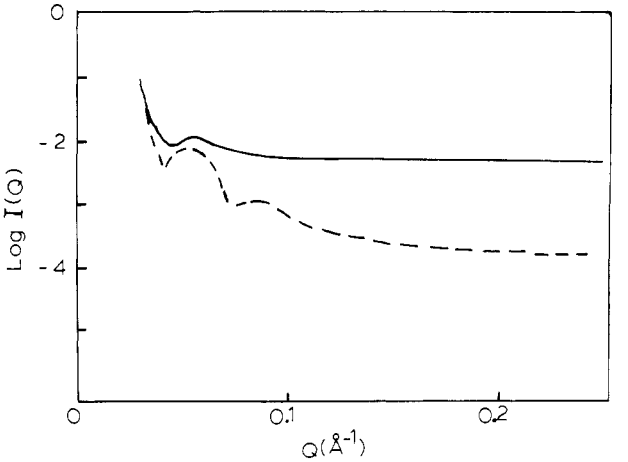

Figure 1. Computed scattering curves for a spherical domain of radius 100 Å with 10% standard deviation in domain size including incoherent background scattering: (—) fully hydrogenous styrene–isoprene copolymer, (- - -) copolymer with deuterated styrene blocks.

Ratio of Signal to Noise. The major contribution to background scattering (noise) in SANS is the incoherent scattering which is particularly large for hydrogenous materials. Inspection of eq 3 shows that absolute values of background scattering depend on block copolymer composition. However, eq 3 may be rearranged such that the relative level of background scattering can be obtained:

$$I(Q) = K(C_f V_p^2 N_p/N)[\langle F_p(Q)\rangle^2 \exp(-\sigma^2 Q^2) + \sigma_{inc} N/(4\pi C_f V_p^2 N_p)] \quad (7)$$

The interference term has been dropped from eq 7, since only single-domain scattering is being considered; additionally the influence of a diffuse domain–matrix boundary is encompassed by the inclusion of the exponential term in σ^2. The relative background scattering is

$$I_{inc} = (N/C_f N_p V_p^2)\sigma_{inc}/4\pi$$

Since

$$N_p V_p = \phi V$$

$$N/V = n$$

$$n = N_A \sum_i \phi_i \rho_i / M_i$$

$$\sigma_{inc} = \phi\sigma_{i,inc} + (1 - \phi)\sigma_{j,inc}$$

then

$$I_{inc} = \frac{N_A[(\phi\rho_D/M_D) + (1 - \phi)\rho_m/M_m]}{C_f V_p \phi} \cdot \frac{[\phi\sigma_{D,inc} + (1 - \phi)\sigma_{m,inc}]}{4\pi} \quad (8)$$

For spherical domain symmetry, eq 8 is calculable since V_p is known unambiguously. Values of contrast factor and incoherent scattering cross sections for styrene–isoprene combinations are given in Table I, while Figure 1 shows the clear advantages of using a partially labeled copolymer to observe single-particle form factor scattering.

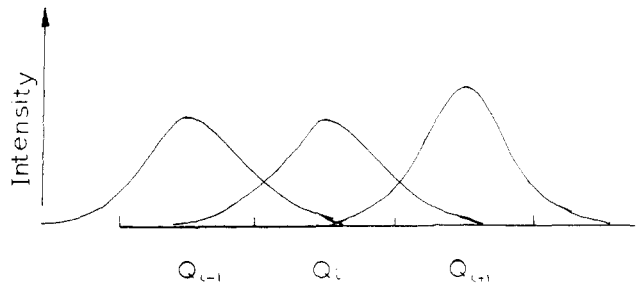

Figure 2. Schematic sketch of the distribution in Q associated with each radial step of discrete Q.

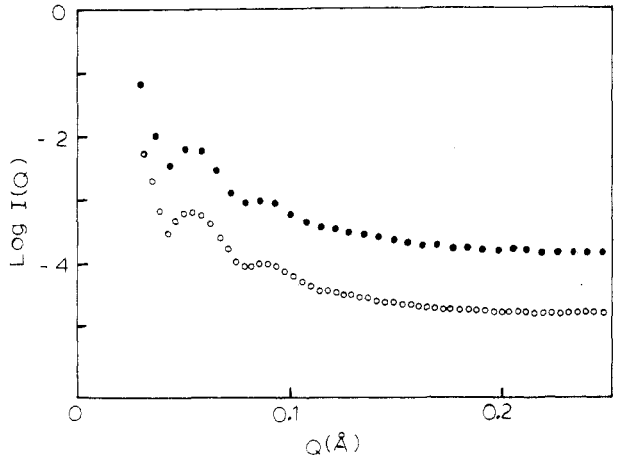

Figure 3. Computed scattering curve for a block copolymer of deuterated styrene and isoprene with spherical domains of radius 100 Å including a distribution in domain size, interface scattering, and relative incoherent background: (●) 1-cm radial steps, (○) 0.5-cm radial steps (shifted down by 1 unit in log $I(Q)$ for clarity).

Table I
Parameters Relevant to Neutron Scattering of Styrene–Isoprene Block Copolymers

	styrene	styrene-d_8	isoprene
ρ, g mL^{-1}	1.05	1.13	0.913
M_i	104	112	68
$10^{24}\sigma_{inc}$, cm^2	696	104.8	679.5
scattering length density, cm^{-2} × 10^{-10}	1.416	6.302	0.289

Wavelength Distribution and Detector Resolution. Neutron beam monochromators on small-angle diffractometers usually provide a beam with $\Delta\lambda/\lambda$ of between 0.05 and 0.1, where $\Delta\lambda$ is the width at half-height of the distribution in wavelengths centered at λ. We have modeled this distribution as a Gaussian with the wavelength distribution translating to a distribution in Q as $Q\Delta\lambda/\lambda$, over which intensity associated with Q, $I(Q)$, is spread.

Detector resolution has been included by dividing the Q range examined into discrete elements which correlate with the finite step sizes used in the radial data analysis procedures currently used.[20] The value of Q associated with each step is Gaussian distributed over that step and the adjacent radial steps, and the intensities in each step are adjusted for this distribution. Figure 2 shows this conception schematically, while Figure 3 is the single-domain scattering for a sphere calculated for 1-cm radial steps and 0.5-cm radial steps commensurate with current detectors. Evidently, the smaller step size improves the resolution of the SPFF maxima and gives greater confidence in obtaining domain dimensions. Inclusion of a wavelength distribution has a negligible effect.

Domain Orientation. Signal-to-noise ratio calculation for lamellar or cylindrical domains is somewhat ambiguous

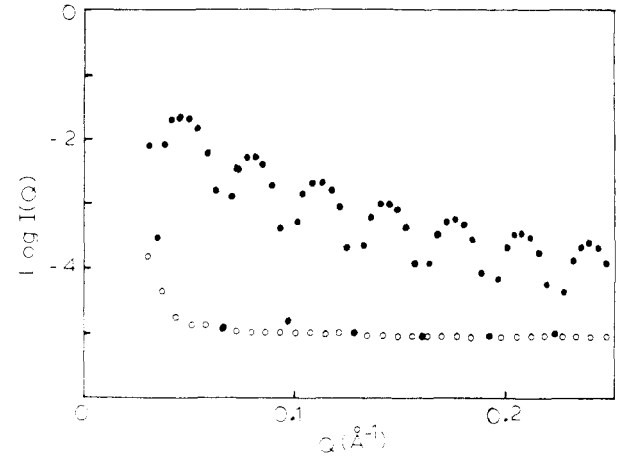

Figure 4. Influence of cylinder orientation on scattered intensity for monodisperse cylinders: (●) β = 90°, (○) β = 45°.

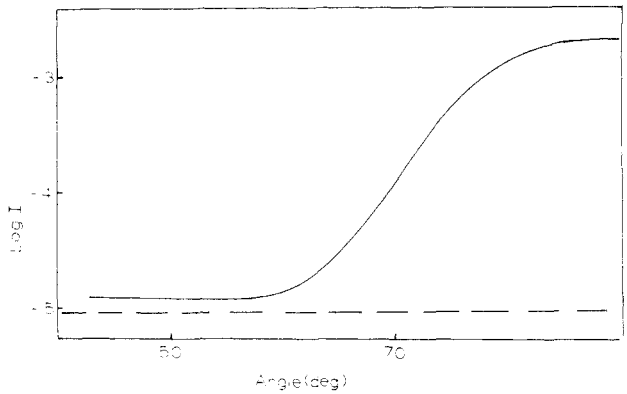

Figure 5. Intensity of first-order maximum for the scattering of cylinder of radius 100 Å as a function of orientation angle β: (- - -) level of incoherent background.

since a value for the lamellar area or cylinder length must be supplied. Additionally, an important factor for these morphologies is their orientation with respect to the scattering vector. Guinier and Fournet[21] provide a general expression for the scattering by particles with a preferred orientation; however, its use depends on a knowledge of the variation of the SPFF with Euler angles for the particle. Since this is not known for block copolymer domains, a simpler method has been used which results from the factorizing of the scattering from anisometric particles into an axial component and a cross-section component,[22] and then using the equation afforded by Fournet[16] for cylindrical particles

$$F_p^2(Q) = \frac{\sin^2 (QH \cos \beta)}{Q^2H^2 \cos^2 \beta} \frac{4J_1^2(QR_c \sin \beta) \sin \beta}{Q^2R_c^2 \sin^2 \beta} \quad (9)$$

where β is the angle between the cylinder axis and **Q** while H is the cylinder length. A distribution about the angle β is emulated by integrating over the range $\beta \pm \pi/2$ rad and normalizing to unit probability over the whole angular range, i.e.

$$\langle F_p(Q)\rangle^2 = \int_{\beta-\pi/2}^{\beta+\pi/2} \frac{\sin^2 (QH \cos \beta)}{Q^2H^2 \cos^2 \beta} \frac{4J_1^2(QR_c \sin\beta)}{Q^2R_c^2 \sin^2 \beta} \sin \beta \, P(\beta) \, d\beta \quad (10)$$

where $P(\beta)$ is the probability associated with an angle β. For lamellae eq 10 is used with H being lamellar thickness and R_c is made very large relative to H; i.e., the lamellar particle becomes a disk. Domain orientation has a severe

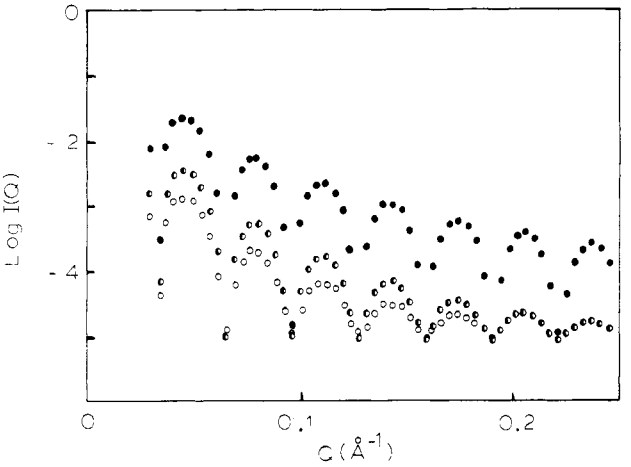

Figure 6. Influence of increasing percentage standard deviation of the angular distribution of cylinder orientation about 90° to the scattering vector: (●) 0% standard deviation, (◐) 10% standard deviation, (○) 30% standard deviation.

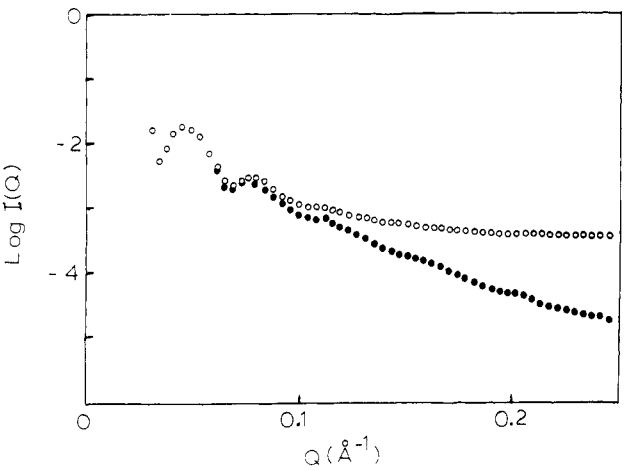

Figure 7. Comparative scattered intensity inclusive of all factors for cylindrical domains of radius 100 Å and length 1000 Å: (○) hydrogenous copolymer, (●) copolymer with deuterated styrene blocks.

influence on SPFF scattering as Figure 4 shows for a cylinder with R_c = 100 Å, H = 1000 Å with β = 90° and 45°. For the latter angle all features except the zeroth-order maximum are deeply buried in the background and contribute a vanishingly small amount to the scattered intensity for $Q \gtrsim 0.05$ Å^{-1}. Figure 5 shows the intensity for the first-order maximum ($Q \simeq 0.05$ Å^{-1}) as a function of β; evidently the range of β wherein the SPFF will be discerned is 90 ± 20°. For a fixed orientation angle of 90°, a broader distribution about this angle increases the damping of the maxima (Figure 6), the effect becoming less significant with increasing breadth of the distribution.

Equation 10 can be modified yet further to account for distributions in both H and R_c of the domain yielding

$$\langle F_p(Q)\rangle^2 = \int_{\beta-\pi/2}^{\beta+\pi/2}\int_{-\infty}^{\infty}\int_{-\infty}^{\infty} \frac{\sin^2(QR\cos\beta)}{Q^2R^2\cos^2\beta} \times \frac{4J_1^2(QR\sin\beta)}{Q^2R^2\sin\beta} \sin\beta\, P(\beta)P(R)P(H)\, d\beta\, dR\, dH \quad (11)$$

Inclusion of distributions in β, R, and H produced an essentially featureless scattering when the percentage standard deviations of each are 10%. Figure 7 shows calculated scattering envelopes for both hydrogenous and deuterated styrene cylinders in a hydrogenous isoprene matrix. Apart from domain–matrix boundary and background scattering, a 10% distribution in R_c and β (β_{mean} = 90°) has been included. The use of deuterated styrene blocks is clearly advantageous for SPFF scattering and the influence of domain boundary; we note that, by contrast to spherical domains, cylindrical domains exhibit three maxima even for the fully hydrogenous copolymer.

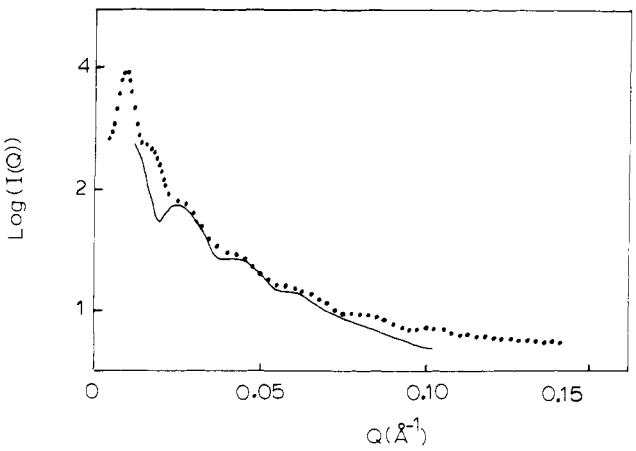

Figure 8. Experimental and computed scattered intensities for cylindrical isoprene domains in a deuterated styrene matrix: (●) experimental, (—) calculated.

Comparison with Experimental Data. Figure 8 shows the agreement between a computed scattering envelope and data obtained for a copolymer with cylindrical isoprene domains in a deuterated styrene matrix. This copolymer (DSI5) has been discussed in detail elsewhere.[10] The details used in computing the curve were a domain radius of 185 Å, a cylinder length of 1800 Å each with a Gaussian distribution with a standard deviation of 10%, while the orientation angle was fixed at 90° with a standard deviation of 6%. The agreement between experiment and model is fair, the intense peak at low Q being due to Bragg scattering.

The widths of both experimental and theoretical maxima are approximately equal, which suggests that the 10% standard deviation in radius is reasonably accurate. However, the calculated curve continues to decay after the experimental curve has settled to a constant value. This may be due to the standard deviation of the angular distribution being too narrow. Using a larger value unfortunately produces a poorer fit of the theoretical maxima to the experimental data. A second source is the calculated background: for cylindrical domains this is dependent on a value for the cylinder length, a larger value giving a lower background, and we may have used too large a value.

A consideration of the section dealing with signal-to-noise ratio reveals that, for a given volume fraction, copolymers with large domains should have a higher signal-to-noise ratio. This is borne out in practice as Figure 9 shows, where data calculated from the model using a cylinder radius of 360 Å and H equal to 3600 Å are compared to the experimental data for copolymer SI5. All distributions in the model were kept exactly as in the previous case and the agreement is generally excellent except, of course, in the region of very low Q where Bragg scattering dominates.

Interdomain Scattering

Transmission electron microscopy of styrene–diene block copolymers reveals long-range order over considerable distances.[1,10] Small-angle scattering also provides evidence for long-range order by virtue of the Bragg maxima at low Q ($Q \leq 0.04$ Å^{-1}). Contour maps of the scattered intensity from these copolymers are usually isotropic[10,14] (lamellar

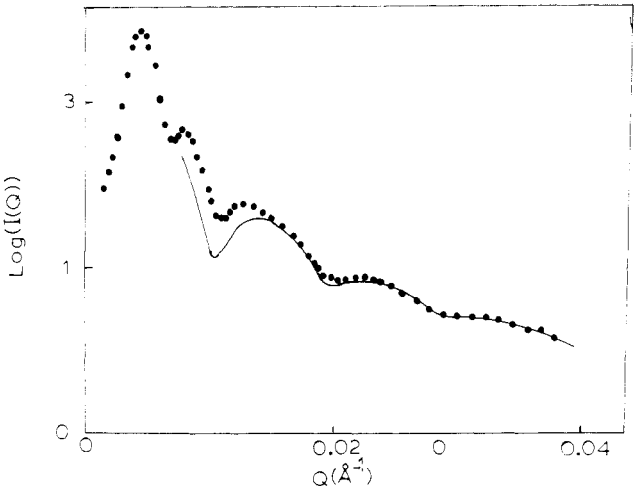

Figure 9. Experimental and computed scattered intensities for a fully hydrogenous styrene–isoprene block copolymer: (●) experimental, (—) calculated.

systems are an exception, see ref 5 and 10). The isotropic scattering is a consequence of the mosaic structure of these block copolymers seen in electron micrographs, wherein different regions are arranged with a differing orientation to the incident wave vector. As a consequence, the small-angle patterns may be considered as the block copolymer analogue of powder diffraction patterns for low molecular weight crystalline materials. Notwithstanding the high degree of perfection in long-range order as viewed by electron microscopy, Bragg peaks in block copolymers observed by small-angle scattering are usually broad, ill-resolved, and absent for $Q > 0.04$ Å^{-1}. Consequently, any model for the interference function must have the following features: (1) long-range order of a regular nature and (2) sufficient disorder that scattering due to the interference function is absent above $Q \approx 0.05$ Å^{-1}.

Theoretical Basis. Some 60 years ago, Zernicke and Prins[23] derived an equation for the scattering envelope of a system with a degree of long-range order. This equation was written in terms of the probability distribution function of particle separation, and its application is difficult since the form of the distribution function is generally unknown. While specific expressions are available for spherical particles (and have recently been applied to SAXS from ionomers[24]), extension to anisometric particles is nontrivial. Such particles have been discussed in terms of a "surrounding function",[22] but again lack of knowledge of the form of this function does not provide any advantage. Because of these difficulties, these methods are not discussed further.

McIntyre et al.[25] were perhaps the first to describe the long-range structure of block copolymers as that of a macrolattice. This term is now frequently used and we have taken this analogy further here. As a basis for calculating the interference function, we have adopted the equations and formalisms used for classical crystalline lattices and expounded in many texts.[26,27] On this basis, the interference function, $A(Q)$, is composed of a structure factor, $S(Q)$, and a lattice factor, $Z(Q)$. The structure factor reduces to a constant value depending on the lattice type and the Miller indices for the lattice planes, while the lattice factor, $Z(Q)$, defines those scattering vectors at which a nonzero scattered intensity will be observed. The latter parameter, $Z(Q)$, includes unit-cell lengths in all three dimensions in its most general form. To simplify and speed the calculation, the stratagem first used by Brown and Taylor[28] has been resorted to. Namely, a simplified one-dimensional form for $Z(Q)$, which assumes that the unit cell has the same dimensions in all directions and that all possible lattice planes are "sampled" by the incident neutron beam. The assumption that all possible lattice planes may be observed is equivalent to stating that the diffraction pattern would be that of a powder; this is supported by the experimental observation of isotropic scattering patterns from block copolymers. Consequently, we include a multiplicity factor, m_{hkl}, characteristic of the number of unit-cell orientations resulting in a particular hkl "Bragg reflection" being observed. On this model $A(Q)$ is

$$A(Q) = \sum^{hkl} S_{hkl}^2 \frac{\sin^2 (N_L d_{hkl} Q/2)}{\sin^2 (d_{hkl} Q/2)} m_{hkl} \qquad (12)$$

with the summation extending over the hkl planes accessible to the specified Q range.

Computation Methods. Combining eq 12 with eq 3 and including the contribution from the domain–matrix boundary then

$$I(\mathbf{Q}) = K\left[\frac{C_f V_p^2 N_p}{N}\langle F_p(\mathbf{Q})\rangle^2 \exp(-\sigma^2\mathbf{Q}^2) \times \sum^{hkl} S_{hkl}^2 \frac{\sin^2 (N_L d_{hkl} Q/2)}{\sin^2 (d_{hkl} Q/2)} m_{hkl} + \frac{\sigma_{inc}}{4\pi}\right] \qquad (13)$$

The essential contributions to eq 3 are retained in a simplified form where the instrumental factor, K, has been omitted and the contrast factor and incoherent scattering have been collected into a background term, B

$$I(\mathbf{Q}) = \langle F_p(\mathbf{Q})\rangle^2 \exp(-\sigma^2\mathbf{Q}^2) \sum^{hkl} S_{hkl}^2 \frac{\sin^2 (N_L d_{hkl} Q/2)}{\sin^2 (d_{hkl} Q/2)} m_{hkl} + B \qquad (14)$$

Equation 14 is that used in the computer program. The type of lattice for which calculations are required is specified as input, i.e., face-centered cubic, hexagonally close packed. Specifying the lattice determines which hkl planes contribute to the diffraction pattern and the values of S_{hkl}^2 and m_{hkl} which are obtained from data in texts on X-ray diffraction[26,27] from crystalline materials. Lattice plane spacings are calculated from the unit-cell side length, which, in its turn, is obtained from an interplanar spacing, d_{int}, provided as input. This d_{int} value is associated with the lattice plane with the smallest combination of Miller indices (excluding the (000) plane) for the specified lattice. Thus, for a face-centered cubic lattice, the plane is (111) while for body-centered cubic it is (110). The maximum value of Q used must be specified since the number of Bragg peaks observable is calculated by comparing the smallest dimension accessible ($\approx 2\pi/Q_{max}$) to the distances associated with each hkl plane. The number of scattering domains in the notional one-dimensional lattice, N_L, does not have a significant effect on the diffraction provide, provided it is larger than about 10. With electron micrographs a typical value for N_L is 25. Instrumental factors such as wavelength distribution and detector resolution are also included.

From eq 14 it is evident that the nature and characteristics of the single-particle form factor will severely influence the observed diffraction pattern. The extreme case would be the coincidence of a minimum in $F_p(\mathbf{Q})$ with a maximum in $A(Q)$, resulting in no excess scattering above the background. Other factors influencing the diffraction

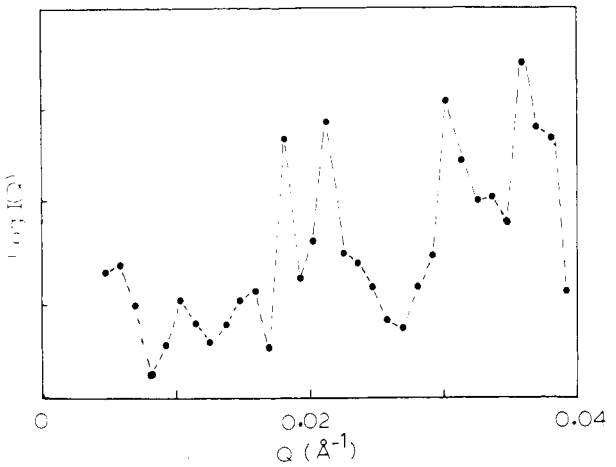

Figure 10. Bragg scattering for 130 Å spheres on a face-centered cubic lattice. Dashed lines are guides to the eye.

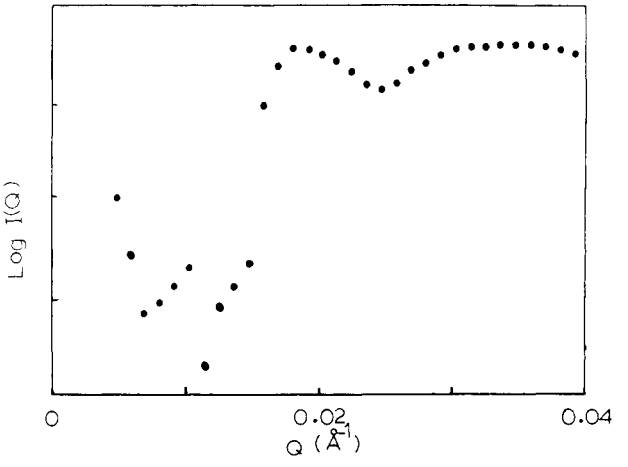

Figure 11. As for Figure 10 with inclusion of a 10% standard deviation in the d_{hkl} values accessible in this Q range.

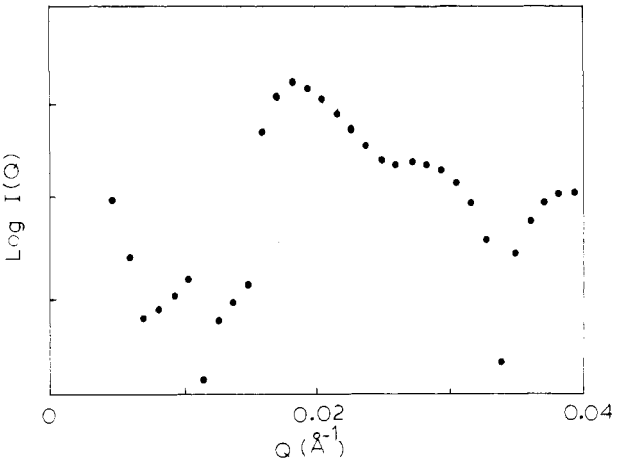

Figure 12. Modulation of Bragg scattering by inclusion of single-particle form factor scattering of a sphere of radius 130 Å.

pattern are a distribution in d_{int} and/or in each d_{hkl} calculated via d_{int}. Distributions in these two parameters have been modeled by using a normalized Gaussian distribution about mean values, the standard deviations being given as input.

A distribution in primary lattice spacing, d_{int}, is equivalent to a distortion of the first kind wherein each domain may not be on a reciprocal lattice node, although the whole assembly retains its long-range order. A distribution of each individual d_{hkl} distance is a distortion of the second kind where the distance between scattering domains has a random variation about a mean value.[29] Incorporating distortions of the first kind into the calculation of $I(\mathbf{Q})$ produces diffraction patterns which in no way resemble those experimentally observed; therefore, this aspect has not been further pursued. Distortions of the second kind produce paracrystallinity, the nature of which has been fully discussed by Vainshtein[29] and Hosemann and Bagchi,[30] and the calculated scattering patterns are akin to those observed.

Results. The modeling of lamellar supramolecular organization has been the subject of a plethora of attempts at modeling the small-angle scattering. Vonk[31] has summarized the attempts used and recent studies have discussed instrumental broadening[32] and evaluation of the correlation function.[33] In view of this, discussion here is limited to cubic packing (spherical domains) and hexagonal close packing (cylindrical domains). Block copolymers with spherical domains present a severe test since the observed diffraction patterns usually have only one broad maximum with indistinct shoulders. High molecular weight block copolymers with cylindrical domains present the converse, the diffraction patterns having very distinct Bragg peaks with strong modulation by the single particle form factor. The results presented here pertain to a detector with 1-cm^2 elements and a wavelength distribution ($\Delta\lambda/\lambda$) of 0.09. These conditions conform to those under which the data were obtained, the resolution in Q being determined by the Q_{max} specified.

Cubic Packing. Notwithstanding the prediction of Leibler[3] that a body-centered cubic arrangement of spherical domains is the most stable, our experimental results suggest a face-centered cubic (fccub) arrangement of spheres prevails. Accordingly, the development of the model will be illustrated by using an fccub lattice, the maximum Q generally being 0.04 Å^{-1} since Bragg peaks have only been observed for $Q < 0.04$ Å^{-1}. Values of d_{int} and sphere radius used are 400 Å and 130 Å, these being typical of the styrene–isoprene copolymers that we investigated. In the absence of single-particle form factor scattering and any distribution in d_{hkl} values, Figure 10 shows the calculated diffraction pattern for an fccub lattice with $d_{111} = 400$ Å. A dashed line through the points serves as a guide to the eye. The strong sharp peaks are the four Bragg maxima evident in this Q range while the secondary maxima are artifacts devolving from the use of a finite number, N_L, of scattering centers. Severe changes are noted if a standard deviation of 0.10 in each d_{hkl} is incorporated. As Figure 11 shows, the four sharp maxima are reduced to two broad maxima of almost equal intensity. Inclusion of the single-particle form factor of the spherical domains produces Figure 12, where now the characteristic feature is one broad peak centered at $Q \approx 0.02$ Å^{-1}, the deep minimum resulting from the severe modulation of $A(Q)$ by $F_p(Q)$. For Q values greater than 0.04, the scattered intensity calculated by this model shows no contribution from the interference function (Figure 13); only the maxima of the SPFF are observed and these are not displaced from the Q values expected for an isolated sphere.

Formal incorporation of incoherent background scattering level is by no means as easy as for the SPFF scattering since multiplicity factors modify the calculated intensity. Therefore, the background scattering has been calculated semiempirically. Intensities for $Q > 0.1$ were calculated in the presence (I_p) and absence (I_A) of an interference function contribution, the latter condition also being in the absence of any background adjustment via eq 8. The incoherent scattering for the SPFF scattering alone

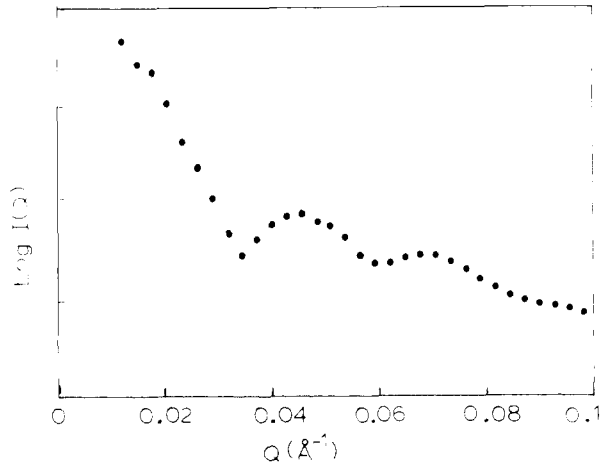

Figure 13. Scattered intensity at higher Q for 130-Å spheres on a face-centered cubic paracrystalline lattice. Only the single-particle form factor scattering is evident.

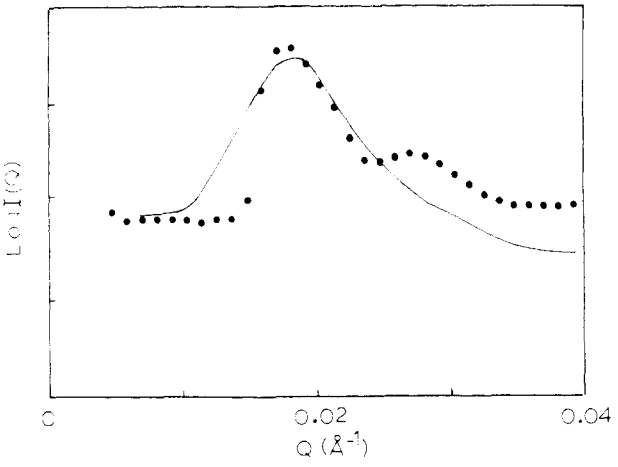

Figure 14. Comparison of calculated scattering of 130-Å spheres on a face-centered paracrystalline lattice with d_{111} = 414 Å and 10% standard deviation in d_{hkl} and sphere radius with experimental data for SI1: (●) calculated results, (—) experimental data.

was calculated from eq 8 and multiplied by the ratio I_p/I_A to provide a value for the background scattering when the interference function plays a role. Typically the value of I_p/I_A so calculated was ca. 80–100.

All of the factors discussed above have been utilized in modeling the small-angle neutron scattering for a styrene–isoprene copolymer, SI1, the experimental results of which have been discussed in earlier publications.[9,10] Only the scattering for $Q \leq 0.04$ Å^{-1} is considered in this section and the comparison between calculated and experimental data is shown in Figure 14. Qualitative agreement between calculation and experiment is obtained in that the position of the main peak is reproduced and a weak secondary peak is obtained in the model. However, the model has notable defects, namely the lack of symmetry in the main peak and the considerably stronger secondary maximum. Increasing the standard distribution of d_{hkl} further produces no better agreement since in these cases only one broad asymmetric maximum is obtained which has no points of similarity with the experimental data.

It is remarked earlier that a body-centered cubic (bccub) structure is the arrangement that is predicted to be the most stable; furthermore, transmission electron microscopy has produced evidence of simple cubic (scub) structures in some cases. Accordingly, these lattices have also been used as a basis to model the small-angle scattering of SI1. For the bccub case, while the main peak occurs at the correct Q position it is too sharp; additionally the secondary maximum is at too low a value of Q. Using a scub lattice as a basis produces a main peak at a Q value which is lower than that observed experimentally for SI1.

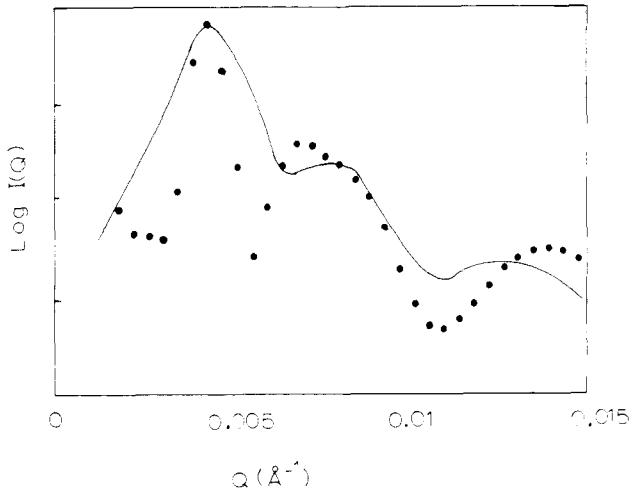

Figure 15. Cylindrical domains of radius 355 Å on a hexagonally close-packed lattice with d_{10} = 1577 Å and a 10% standard deviation in d_{hk} and cylinder radius: (●) calculated results, (—) experimental data for SIS.

Hexagonally Close Packed. Styrene–isoprene copolymers with cylindrical domains have been modeled by using a hexagonally close-packed lattice as a basis for the Bragg scattering. The particular copolymer modeled is SI5 which has two Bragg peaks at very low Q and a suggestion of a third at a somewhat higher (but still small) value of Q[10]. Figure 15 compares the calculated scattered intensity with the observed data for $Q < 0.04$ Å^{-1}.

As for the case of spherical domains of SI1 discussed above, we again have qualitative agreement between theory and experiment. The positions in Q space of the first and second Bragg peaks are reasonably accurately reproduced; that of the third is well displaced from the experimental observation. Furthermore, the first Bragg peak is considerably sharper and all calculated peaks are of greater amplitude than those actually observed; nevertheless, the relative magnitude of the Bragg peak intensities is the same for both model and measured small-angle neutron scattering data. Transmission electron micrographs generally show that cylindrical domains have a very high degree of long-range order; therefore, there is no basis for using a larger standard deviation of each d_{hkl}; in any case, broader distributions result in loss of Bragg peak resolution. However, a narrower distribution of d_{hkl} values narrows the Bragg peak width and any agreement with experimental data is lost.

Evidently the single particle form factor exercises a strong influence on $A(Q)$ and a factor we have not included (due to excessive computing time) is the orientation of the cylindrical domains with respect to **Q**. Referring back to the results obtained when considering only the SPFF, then a distribution about $\beta = 90°$ does not displace the SPFF maxima and minima but does considerably reduce the intensity. Hence, the inclusion of a suitable degree of domain orientation may produce agreement between the amplitudes of calculated and experimental Bragg peaks; it will not, unfortunately, influence the breadth of the maxima.

Conclusions

We have described attempts at modeling the small-angle neutron scattering from microphase-separated block copolymers. The component of the scattered intensity due to single-domain scattering can be factorized from the

expression and treated separately. Instrumental factors have been included, especially the detector resolution, as well as the influence of domain size distribution and diffuse boundary layer. The latter two factors have been discussed elsewhere in relation to small-angle X-ray scattering, and in relation to their influence the effect of detector resolution in the Q range used for observing single-domain scattering is slight. Of greater moment are the incoherent neutron scattering and domain orientation, the latter being equally applicable to small-angle X-ray scattering. For fully hydrogenous copolymers, incoherent scattering may be so large that only one maximum may be resolvable. However, for high molecular weight block copolymers, i.e., large domains, the single-domain scattering occurs in a lower range of Q and with greater amplitude; thus, the incoherent scattering is less important, enabling such scattering to be observed even for hydrogenous polymers. The net conclusion however is that using a partly deuterated block copolymer improves the prospect of observing single-domain scattering. A novel feature has been the attempt to include the domain orientation. Evidently, the intensity of scattering is severely attenuated if lamellar or cylindrical domains are not orientated correctly with respect to the scattering vector. While the orientation does not change the Q positions of the maxima, the reduction in intensity will clearly reduce the probability of their observation, especially where considerable incoherent scattering prevails. Furthermore, since the interference function scattering is *always* modulated by the SPFF scattering, then some domain orientations will not contribute in any way to the small-angle scattering signal. By adjustment of all of these factors, then a reasonable agreement with experimental SANS data can be obtained.

Long-range structure of the domains has been modeled on the basis of a paracrystalline lattice, i.e., one wherein each lattice plane spacing is distributed about a mean value. While qualitative agreement of the model with SANS data has been obtained, evident disagreements still prevail. Notably calculated peak widths are much narrower than observed experimentally. Peak widths have been associated with "grain" sizes and therefore the number of scattering centers as well as the distribution width of d_{hkl} will influence the observed peak width. A smaller number of scattering centers will give a broader peak; however, this is accompanied by additional small oscillations between the main peaks which do not improve the fit of model to experimental data. Comparison of results with an equilibrium theory in an earlier paper showed that spherical domain separation does not have equilibrium behavior. Unfortunately this aspect of block copolymer microphase structure cannot be clarified by the modeling described here, since the use of the model is predicated on having values for d_{int} in the final phase-separated state. Observation of the mechanism of phase separation may provide suitable data on the equilibrium or nonequilibrium aspects of the domain separation.

The programs developed may be used on any machine, including microcomputers;[34] since they consist of a series of subroutines, they may be easily adapted for other types of particles on different lattices. Additionally, by suitable modification of the subroutine for calculation of background scattering, the programs can be used for calculation of small-angle X-ray scattering patterns. Similarly, the use of Gaussian distributed quantities can be replaced by any type of distribution more descriptive of the system of interest. Apart from using the programs to assess distribution parameters from experimental data, they have been used to optimize experimental arrangements (e.g., deuteration, Q resolution, Q range, etc.), to observe particular features, for example the resolution of Bragg peaks in uniaxial extension or the attenuation in scattering for "large" Q values.

Acknowledgment. We thank the SERC for financial support of the research on which this work is based and for the provision of neutron beam facilities. The assistance of staff at AERE Harwell, U.K., and Institut Laue-Langevin, Grenoble, France, in executing experiments was also invaluable.

Glossary of Symbols

$A(Q)$	interparticle interference function
C_f	contrast factor
D	characteristic domain dimension (radius of sphere or cylinder, thickness of lamellar domain)
d_{hkl}	hkl lattice plane spacing
$F_p(\mathbf{Q})$	single-particle form factor
H	cylinder length
$I(\mathbf{Q})$	intensity scattered at scattering vector $\mathbf{Q}$
J_n	Bessel function of the first kind of order n
K	composite factor containing instrumental factors, e.g. neutron flux, sample–detector separation, etc.
L	lamellar thickness
M_i	molar mass of monomer unit i
m_{hkl}	multiplicity factor
N	number of scattering nuclei in scattering volume
N_A	Avogadro's number
N_L	number of scattering centers in one-dimensional lattice
N_p	number of domains in scattering volume
$P(p)$	normalized Gaussian distribution of parameter p
$\mathbf{Q}$	scattering vector $(4\pi/\lambda) \sin(\theta/2)$
R_c	cylinder radius
R_s	sphere radius
$S(Q)$, S_{hkl}	structure factor
t	interfacial layer thickness
V	scattering volume
V_p	scattering particle volume
$Z(Q)$	lattice factor
β	angle between scattering vector and cylinder axis
ϕ	volume fraction of domain forming component in block copolymer
ρ	density
σ	standard deviation characterizing segment density distribution of domain–matrix interface
σ_{inc}	incoherent scattering cross section
$d\sigma_c/d\Omega$	differential coherent scattering cross section
D	subscript D signifies domain forming polymer
m	subscript m signifies matrix forming polymer
hkl	Miller indices

Registry No. (Styrene)·(isoprene) (copolymer), 25038-32-8; neutron, 12586-31-1.

References and Notes

(1) Gallot, B. R. M. *Adv. Polym. Sci.* **1978**, *29*, 85.
(2) Helfand, E.; Wasserman, Z. R. In "Developments in Block Copolymers"; Goodman, I., Ed.; Applied Science Publishers: London, 1982; Vol. 1, Chapter 4.
(3) Leibler, L. *Macromolecules* **1980**, *13*, 1602.
(4) Hong, K. M.; Noolandi, J. *Macromolecules* **1983**, *16*, 1083.
(5) Hashimoto, T.; Shibayama, M.; Kawai, H. *Macromolecules* **1980**, *13*, 1237.
(6) Hashimoto, T.; Fujimura, M.; Kawai, H. *Macromolecules* **1980**, *13*, 1660.
(7) Fujimura, M.; Hashimoto, H.; Kurahashi, K.; Hashimoto, T.; Kawai, H. *Macromolecules* **1981**, *14*, 1196.

(8) Shibayama, M.; Hashimoto, T.; Kawai, H. *Macromolecules* **1983**, *16*, 1434 and cognate references.
(9) Richards, R. W.; Thomason, J. L. *Polymer* **1981**, *22*, 581.
(10) Richards, R. W.; Thomason, J. L. *Macromolecules* **1983**, *16*, 982.
(11) Richards, R. W.; Thomason, J. L. *Polymer* **1983**, *24*, 1089.
(12) Berney, C. V.; Cohen, R. E.; Bates, F. S. *Polymer* **1982**, *23*, 1222.
(13) Bates, F. S.; Cohen, R. E.; Berney, C. V. *Macromolecules* **1982**, *15*, 589.
(14) Bates, F. S.; Berney, C. V.; Cohen, R. E. *Macromolecules* **1983**, *16*, 1101.
(15) Rayleigh, Lord. *Proc. R. Soc. London, Ser. A* **1914**, *90*, 219.
(16) Fournet, G. *Bull. Soc. Franc. Mineral. Cristallogr.* **1951**, *74*, 39.
(17) Schelten, J.; Schmatz, W. J. *Appl. Crystallogr.* **1980**, *13*, 385.
(18) Goyal, P. S.; King, J. S.; Summerfield, G. C. *Polymer* **1983**, *24*, 131.
(19) Ruland, W. "Colloque Franco-Americain sur la Diffusion des Rayons-X et des Neutrons aux Petits Angles par les Polymeres", Strasbourg, 1980.
(20) Ghosh, R. E. "A Computing Guide for Small Angle Scattering Experiments"; Institut Laue-Langevin: Grenoble, 1981; Report No. 81GH29T.
(21) Guinier, A.; Fournet, G. "Small Angle Scattering of X-Rays"; Wiley: New York, 1955.
(22) Porod, G. In "Small Angle X-ray Scattering"; Glatter, O., Kratky, O., Eds.; Academic Press: London, 1982; Chapter 2.
(23) Zernicke, F.; Prins, J. A. *Z. Phys.* **1927**, *41*, 184.
(24) Yarusso, D. J.; Cooper, S. L. *Macromolecules* **1983**, *16*, 1871.
(25) McIntyre, D.; Campus-Lopez, E. *Macromolecules* **1970**, *3*, 322.
(26) Schultz, J. M. "Diffraction for Materials Scientists"; Prentice-Hall: Englewood Cliffs, NJ, 1982.
(27) Cullity, B. E. "Elements of X-Ray Diffraction", 2nd ed.; Addison-Wesley: Reading, MA, 1978.
(28) Brown, B. L.; Taylor, T. J. *Appl. Polym. Sci.* **1974**, *18*, 1385.
(29) Vainshtein, B. K. "Diffraction of X-Rays by Chain Molecules"; Elsevier: Amsterdam, 1966.
(30) Hosemann, R.; Bagchi, S. N. "Direct Analysis of Diffraction by Matter"; North-Holland: Amsterdam, 1962.
(31) Vonck, C. G. In "Small Angle X-Ray Scattering"; Glatter, O., Kratky, O., Eds.; Academic Press: London, 1982; Chapter 13.
(32) Harrison, I. R.; Kozmiscki, S. J.; Varnell, W. D.; Wang, J. I. *J. Polym. Sci., Polym. Phys. Ed.* **1981**, *19*, 487.
(33) Strobl, G. R.; Schneider, M. *J. Polym. Sci., Polym. Phys. Ed.* **1980**, *18*, 1343.
(34) Source listings of programs may be obtained from the authors.

Surface Pressure from Block Copolymers with One Block Forming a Monolayer and the Other Block Dangling in Solution†

Steve Granick*

Physique de la Matière Condensée,‡ Collège de France, 75231 Paris Cedex 05, France

Jean Herz

Centre de Recherches sur les Macromolécules (C.N.R.S.), 67083 Strasbourg Cedex, France.
Received April 23, 1984

ABSTRACT: Surface pressure has been measured as a function of surface concentration for monolayers of poly(dimethylsiloxane)–polystyrene (PDMS–PS) diblock copolymers, PDMS–poly(α-methylstyrene) (PDMS–PαMS) multiblock copolymers, and the respective homopolymers, spread on the surface against air of tricresyl phosphate at 26 °C. A sparingly soluble monolayer was formed by PDMS homopolymer. No surface pressure was associated with either PS or PαMS homopolymer; these appeared to pass into bulk solution. For the block copolymers, at low surface concentrations the surface pressure was indistinguishable from that for PDMS homopolymer at the same concentration of PDMS. At higher concentrations the surface pressure exceeded this value, to an extent which increased with increasing surface concentration of PS or PαMS. The supplemental surface pressure from dangling chains was calculated by subtraction. The findings are in qualitative agreement with theoretical predictions by de Gennes, Alexander, and Cantor that osmotic interactions between polymer chains dangling into a liquid from an interface contribute substantially to the reduction of surface tension. Idealizations in the theoretical models are noted.

Introduction

Block copolymers are amphiphilic and can behave as surfactants. At small concentrations in a liquid they can concentrate at the surface, lowering the surface tension considerably.[1] This property finds technological applications in blends of immiscible polymeric liquids.[2] At higher concentrations, block copolymers can assemble into micelles[3] or other organized structures.[4] They can bring into solution material that is otherwise insoluble.[5] The outlook for understanding this behavior appears in some respects more favorable for uncharged amorphous block copolymers than for surfactants of the traditional type.[6] The absence of charges simplifies the situation compared to that for surfactants with polar heads. And in contrast to small nonionic surfactants, the long length of flexible polymers makes possible predictions based on the statistical thermodynamics of homopolymer solutions, which is relatively well understood. Study of block copolymers for the elucidation of surfactant action has been urged.[6-9]

A theory for the interaction between polymer chains dangling from one end into a liquid has been proposed by de Gennes,[6] Alexander,[7] and Cantor.[8] A parallel can be drawn between the dangling chains and the tails of conventional small amphiphilic molecules. In the theoretical models, at a water–oil interface a hydrophilic and a hydrophobic block straddle the interface, each dangling into the liquid for which it has affinity; at a liquid–air interface one of the blocks adsorbs tightly, riding on the surface as a buoy which traps the other. In both cases there is considered to exist a well-defined surface phase of polymer in thin three-dimensional solution, but attached to the

† We take pleasure in dedicating this paper to Pierre Thirion on the occasion of his retirement.

* To whom correspondence may be addressed at Polymer Group and Department of Ceramic Engineering, University of Illinois, Urbana, IL 61801.

‡ Équipe de recherche associé au C.N.R.S.

0024-9297/85/2218-0460$01.50/0